Research Article

Molecular Cancer Therapeutics

Alisol B, a Novel Inhibitor of the Sarcoplasmic/Endoplasmic Reticulum Ca^{2+} ATPase Pump, Induces Autophagy, Endoplasmic Reticulum Stress, and Apoptosis

Betty Y.K. Law[1,2,4,5], Mingfu Wang[3], Dik-Lung Ma[1,2], Fawaz Al-Mousa[6], Francesco Michelangeli[6], Suk-Hang Cheng[4,5], Margaret H.L. Ng[4,5], Ka-Fai To[4,5], Anthony Y.F. Mok[4,5], Rebecca Y.Y. Ko[1], Sze Kui Lam[1], Feng Chen[3], Chi-Ming Che[1,2], Pauline Chiu[1,2], and Ben C.B. Ko[4,5]

Abstract

Emerging evidence suggests that autophagic modulators have therapeutic potential. This study aims to identify novel autophagic inducers from traditional Chinese medicinal herbs as potential antitumor agents. Using an image-based screen and bioactivity-guided purification, we identified alisol B 23-acetate, alisol A 24-acetate, and alisol B from the rhizome of *Alisma orientale* as novel inducers of autophagy, with alisol B being the most potent natural product. Across several cancer cell lines, we showed that alisol B–treated cells displayed an increase of autophagic flux and formation of autophagosomes, leading to cell cycle arrest at the G_1 phase and cell death. Alisol B induced calcium mobilization from internal stores, leading to autophagy through the activation of the CaMKK-AMPK-mammalian target of rapamycin pathway. Moreover, the disruption of calcium homeostasis induces endoplasmic reticulum stress and unfolded protein responses in alisol B–treated cells, leading to apoptotic cell death. Finally, by computational virtual docking analysis and biochemical assays, we showed that the molecular target of alisol B is the sarcoplasmic/endoplasmic reticulum Ca^{2+} ATPase. This study provides detailed insights into the cytotoxic mechanism of a novel antitumor compound. *Mol Cancer Ther; 9(3); 718–30. ©2010 AACR.*

Introduction

Autophagy is an evolutionarily conserved mechanism by which cellular proteins and organelles are eliminated by the lysosomal degradation pathway (1). This is a multistep process that involves the formation, expansion, and fusion of an isolated membrane to form double-membraned vesicles known as autophagosomes, by which cytoplasmic materials are sequestered and subsequently fused with the lysosome for degradation (2). Autophagy is constitutively active at a low basal level *in vivo* and is important for cellular homeostasis by removal of damaged or superfluous organelles and proteins. Defects in the autophagic pathway is associated with DNA damage, chromosome instability (3), and increased incidence of malignancies (4), whereas an intact autophagic pathway is necessary for longevity (5). Under nutrient deprivation, growth factor deprivation, and hypoxia, autophagy acts as an alternative cellular energy source by degrading intracellular materials and generating free amino and fatty acids to fuel mitochondrial ATP production (2). Uncontrolled upregulation of autophagy might lead to autophagic cell death (type II programmed cell death; ref. 6).

Emerging evidence suggests that modulators of autophagy may have therapeutic potential. For instance, rapamycin, an inducer of mammalian target of rapamycin (mTOR)–dependent autophagy, is effective in treating fruit fly and mouse models of Huntington's disease through increased autophagic clearance of mutant huntingtin fragments (7). Recently, a small-molecule screen revealed additional new chemical entities that attenuate mutant huntingtin-fragment toxicity through an mTOR-independent mechanism (8). Modulators of autophagy may also play a role in cancer therapy. It has been proposed that for certain tumors undergoing protective autophagy in response to chemotherapy, inhibitors of autophagy may sensitize cancer cells to therapeutic agents. Moreover, autophagic inducers may promote autophagic cell death in tumors directly or augment the efficacy of chemotherapeutic agents when used in

Authors' Affiliations: [1]Department of Chemistry, [2]Open Laboratory of Chemical Biology of the Institute of Molecular Technology for Drug Discovery and Synthesis, and [3]School of Biological Sciences, The University of Hong Kong; and [4]Department of Anatomical and Cellular Pathology and [5]The State Key Laboratory in Oncology in Southern China, The Chinese University of Hong Kong, Hong Kong, China; and [6]School of Biosciences, University of Birmingham, Birmingham, United Kingdom

Note: Supplementary material for this article is available at Molecular Cancer Therapeutics Online (http://mct.aacrjournals.org/).

Corresponding Author: Ben C.B. Ko, The Chinese University of Hong Kong, Room 38019, 1st/Floor, Clinical Sciences Building, Prince of Wales Hospital, Hong Kong, Hong Kong. Phone: 852-26321294; Fax: 852-26376274. E-mail: benko@cuhk.edu.hk and Pauline Chiu, Phone: 852-28598949; E-mail: pchiu@hku.hk.

doi: 10.1158/1535-7163.MCT-09-0700

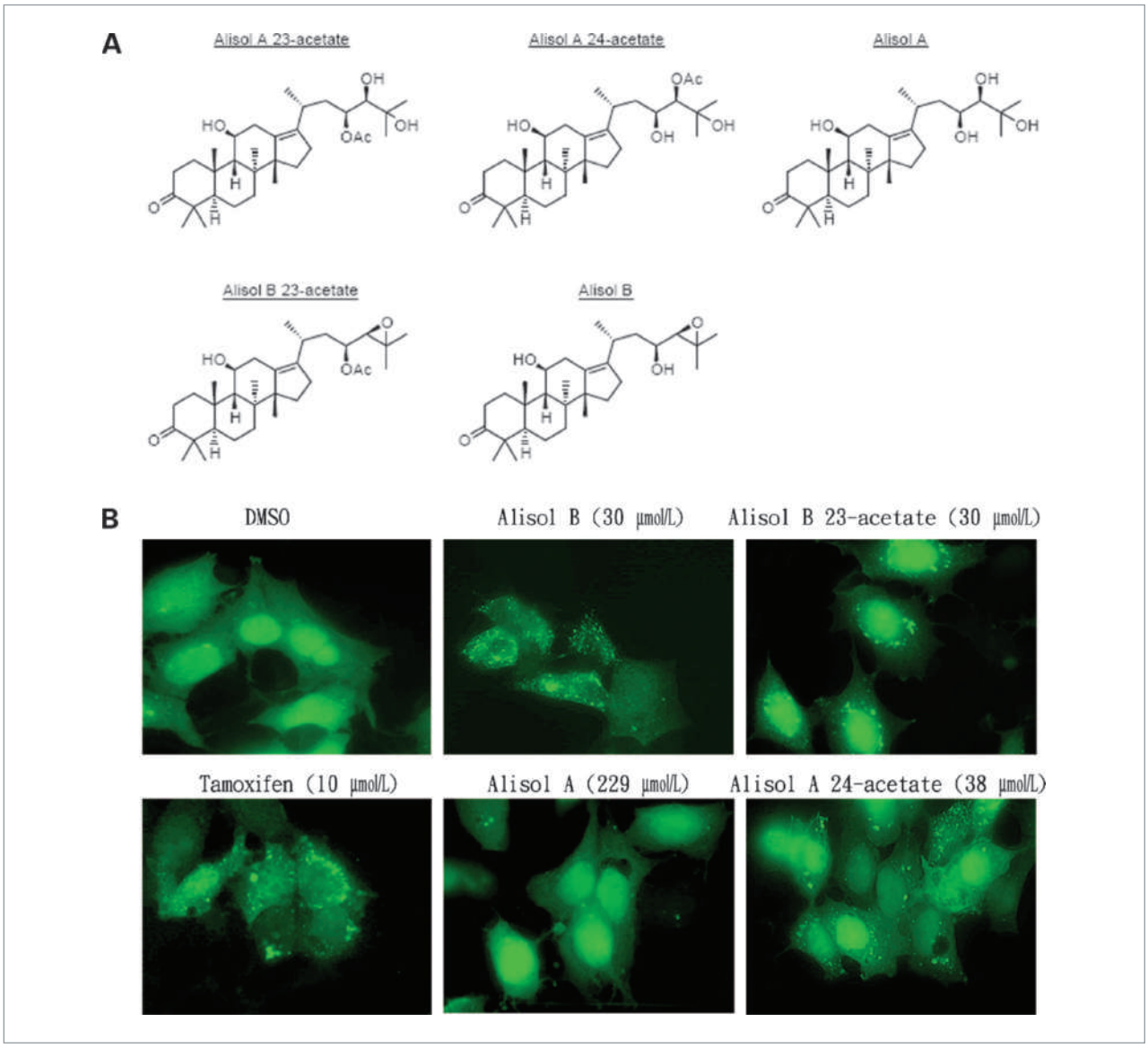

Figure 1. Alisol B induces cytotoxicity and autophagy in multiple cancer cell lines. A, structure of alisol B and its structural analogues. B, induction of autophagy by alisol B and related compounds. MCF-7 cells expressing GFP-LC3 were treated with the indicated compounds at their respective IC_{50} for 24 h. Tamoxifen (10 μmol/L) was used as a positive control. The concentration of DMSO used to dissolve the compound is 0.03%. Magnification, ×63.

combination (9). Consistent with the latter hypothesis, several clinically approved or experimental antitumor agents induced autophagy-related cell death (9–12). However, whether autophagy is a prosurvival mechanism in response to the cytotoxicity of these agents or directly responsible for cell death in these cells remains to be characterized.

In this study, we set out to identify novel inducers of autophagy and evaluate their potential use as antitumor therapeutics. Through screening of our natural product collections and extracts from traditional Chinese medicinal herbs, we have identified alisol B as a novel enhancer of autophagy. We herein present evidence that alisol B increased autophagic flux in several cell lines derived from different tumors, leading to cell cycle arrest and cell death. Alisol B induced autophagy through mobilizing intracellular calcium and activating the CaMKK-AMPK-mTOR signaling cascade as a cell protective response toward alisol B–induced cytotoxicity. Furthermore, we show that alisol B induced unfolded protein responses (UPR) and apoptotic cell death. We also present evidence that the molecular target of alisol B is the sarcoplasmic/endoplasmic reticulum (ER) Ca^{2+} ATPase (SERCA) pump. Together, our work provides novel insights into

the molecular mechanism of alisol B–induced cell death, which is essential for the further development of this compound into an antitumor agent.

Materials and Methods

Chemicals, Plasmids, Small interfering RNAs, and Antibodies

All compounds were purchased from Sigma unless otherwise stated. Thapsigargin, compound C, BAPTA/AM, E64D, pepstatin A, staurosporine, and STO-609 were obtained from Calbiochem. Alisol B and alisol B 23-acetate were purchased from Wako Pure Chemical Industries. Alisol A and alisol A 24-acetate were from Herbstandard, Inc. Antibodies against p70S6 kinase, phospho-p70S6 kinase (Thr389), AMPKα, phospho-AMPKα (Thr172), eIF2α, phospho-eIF2α (Ser51), poly ADP ribose polymerase, beclin1, and PERK were purchased from Cell Signaling Technology, Inc. CHOP, GRP78, and ATF4 antibodies were purchased from Santa Cruz Biotechnology. Anti-LC3 antibody was from Medical & Biological Laboratories Co., Ltd. Anti-p27 antibodies were from DAKO. Anti-phospho-PERK (Thr980) antibodies were from BioLegend. Anti–β-actin antibody was from Sigma. pEGFP-LC3 reporter plasmid was a gift from Prof. Tamotsu Yoshimori (Osaka University, Osaka, Japan). pATF6-Luc was kindly provided by Dr. DY Jin (The University of Hong Kong, Hong Kong, China; ref. 13). *SMART*pool small interfering RNAs targeting beclin1 and nontargeting control were obtained from Dharmacon.

Cell Culture

All cells were obtained from the American Type Culture Collection unless otherwise specified. Immortalized wild-type and ATG7-deficient mouse embryonic fibroblasts were kindly provided by Prof. Masaaki Komatsu (Juntendo University School of Medicine, Tokyo, Japan). C666-1 cells and PC3 cells were gifts from Prof. KW Lo and Prof. KM Lau, respectively (The Chinese University of Hong Kong, Hong Kong, China). Alisol A, alisol B, alisol A 24-acetate, and alisol B 23-acetate, were dissolved in DMSO before adding to the culture medium.

Quantification of GFP-LC3 Puncta

Cells were fixed with 4% paraformaldehyde, permeabilized with methanol, and nuclei were stained with 4′,6-diamidino-2-phenylindole. To quantify autophagy, the percentage of cells with punctuate GFP-LC3 fluorescence was calculated by counting the number of the cells showing the punctuate pattern of GFP-LC3 in green fluorescent protein (GFP)–positive cells. A minimum of 150 cells from three randomly selected fields were scored per set of conditions per experiment.

Cytotoxicity Assays

Cell viability was measured using MTT as previously described (14).

Transmission Electron Microscopy

Cells were fixed overnight with 2.5% glutaraldehyde followed by a buffer wash. Samples were postfixed in 1% OsO_4 and embedded in Araldite 502. Ultrathin sections were doubly stained with uranyl acetate and lead citrate, and analyzed using the Philips CM 100 transmission electron microscope at a voltage of 80 kV.

Analysis of Cell Cycle Distribution and Apoptosis

Cells treated with alisol B were analyzed after the indicated times by multiparametric flow cytometry using the Annexin V and 7-ADD assay (BD Biosciences) according to the manufacturer's instructions; to analyze DNA content, cells were stained with propridium iodide (Sigma-Aldrich). Flow cytometry was carried out using a FACSCalibur flow cytometer (BD Biosciences). Data acquisition and analysis were done with CellQuest (BD Biosciences).

Table 1. Cytotoxicity of alisol B and related compounds against different tumor cells

Compounds	IC_{50} (μmol/L)			
Cell type	Alisol B 23-acetate	Alisol B	Alisol A 24-acetate	Alisol A
Hep3B	43.4 ± 0.1	38.3 ± 5.5	19.1 ± 1.0	162.1 ± 3.6
HepG2	24.8 ± 0.8	20.6 ± 4.2	35.7 ± 0.1	154.5 ± 7.3
HeLa	21.0 ± 2.0	24.3 ± 1.6	27.2 ± 4.6	153.2 ± 1.5
SK-BR-3	42.8 ± 2.0	40.0 ± 0.3	96.8 ± 4.8	210.8 ± 3.1
MDA-MB-231	46.8 ± 7.2	48.7 ± 2.4	93.0 ± 2.6	216.4 ± 2.0
MCF-7	28.9 ± 1.3	29.9 ± 2.6	38.2 ± 1.5	229.0 ± 9.6
PC3	46.9 ± 3.4	38.1 ± 2.3	78.7 ± 1.3	175.1 ± 6.1
C666-1	31.0 ± 2.3	24.7 ± 1.2	70.5 ± 2.8	172.7 ± 6.1

NOTE: Cell viability was measure at 48 h after treatment. The IC_{50} (mean ± SEM) was determined graphically from the survival curves.

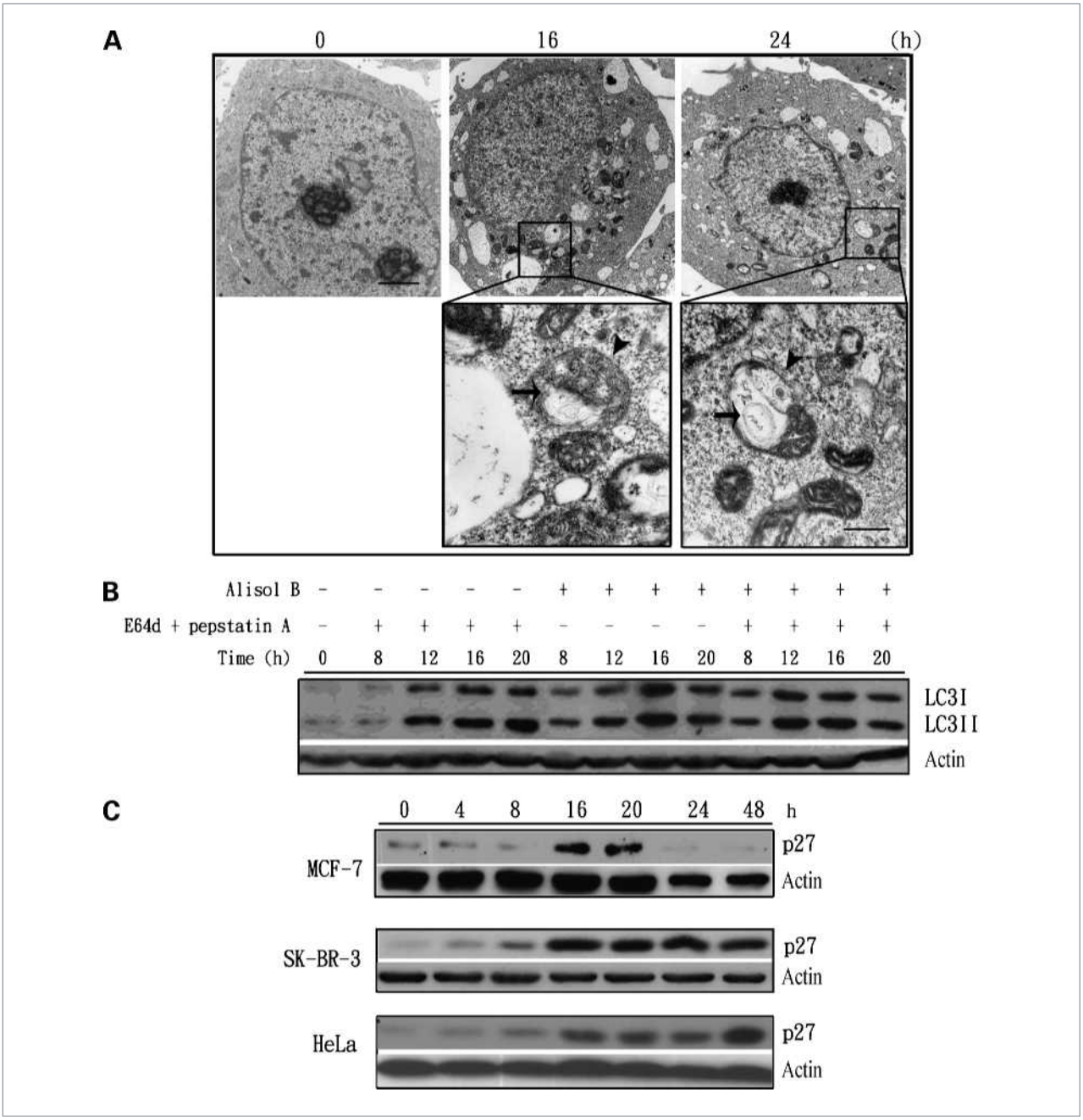

Figure 2. A, alisol B induces the formation of autophagosomes. Representative electron micrographs showing the ultrastructures of MCF-7 cells treated with alisol B (30 μmol/L) at indicated times. Arrowheads, double-membraned autophagosomes. Arrows, engulfed organelles. Bar, 2 μm. B, alisol B induces autophagic flux. MCF-7 cells were treated with alisol B (30 μmol/L) and lysosomal protease inhibitors (10 μg/mL), either alone or in combination, for the indicated time. Cell lysates were analyzed by Western blot for LC3 conversion (LC3-I, 18 kDa; LC3-II, 16 kDa) and β-actin, respectively. C, induction of p27 by alisol B. MCF-7, SK-BR-3, and HeLa cells were treated with alisol B at its IC_{50} concentration. Cell lysates were analyzed by Western blot for p27 and β-actin, respectively.

Luciferase Reporter Assay

MCF-7 cells were transiently transfected with pATF6-Luc and pCMV-*Renilla* (Promega), and treated with the test compounds. Reporter assays were done using the Dual-Luciferase kit (Promega). Luciferase and Renilla luciferase activity was measured with a Victor^3 Multilabel Plate Reader (Perkin-Elmer).

Reverse Transcription-PCR Analysis of Xbp-1 mRNA Splicing

Total RNA was extracted. First-strand cDNA was synthesized using the High-Capacity RNA-to-cDNA Master Mix (Applied Biosystems). To detect human spliced and unspliced Xbp-1 mRNA, PCR was done using primers 5′-CTGGAACAGCAAGTGGTAGA-3′ and 5′-CTGGGT-

Table 2. Quantitative analysis of cell cycle distribution (% of total ± SEM) of MCF-7 cells treated with alisol B

Time (h)	0	8	16	24	48
G_1	41.6 ± 3.8	45.1 ± 1.4	79.2 ± 1.3	88.3 ± 0.7	93.1 ± 2.1
S	36.4 ± 2.2	40.7 ± 0.9	6.9 ± 1.1	4.0 ± 0.5	0.8 ± 0.2
G_2-M	22.0 ± 1.7	14.2 ± 0.9	13.9 ± 1.3	7.7 ± 0.3	6.1 ± 1.9

CCTTCTGGGTAGAC-3′ as described in ref. (15). Spliced (398 bp) and unspliced (424 bp) Xbp-1 fragments were separated by electrophoresis in a 2% agarose gel with DNA bands stained with ethidium bromide and photographed.

Virtual Ligand Docking

Molecular docking was done using the ICM-Pro 3.6-1 program (Molsoft; ref. 16). The protein crystal structure of rabbit SERCA1A with bound thapsigargin (PDB code: 2AGV) was downloaded from the protein data bank as a basis for modeling. The complexes were evaluated with a full-atom ICM ligand binding score (17) that has been previously derived from a multireceptor screening benchmark as a compromise between approximated Gibbs free energy of binding and numerical errors. As a reference, molecular docking of the known SERCA pump inhibitor, thapsigargin, showed a score of −32.

The Measurement of SERCA Activity

Purified Ca^{2+} ATPase was prepared from female rabbit hind leg muscle (18). ATPase activity was determined using the enzyme-coupled method utilizing pyruvate kinase and lactate dehydrogenase as previously described (19). Porcine brain microsomes were prepared as described in ref. (20). Due to the relatively low level of Ca^{2+}ATPase activity in these microsomal membranes, the rate of Ca^{2+}-dependent ATP hydrolysis were measured using the more sensitive phosphate liberation assay, described in ref. (21). All SERCA inhibition data were fitted to the allostearic dose versus effect equation using Fig P (Biosoft):

$$\text{Activity} = \text{minimum activity} + (\text{maximum activity} - \text{minimum activity})/(1 + ([\text{I}]/IC_{50})^{P}).$$

Results

A GFP-LC3 Screening Assay to Identify Inducers of Autophagy

To identify potential small-molecule therapeutics for cancer that targeted the autophagic pathway, we took advantage of the GFP-LC3 reporter system to screen for novel inducers of autophagy (17). We transiently transfected and expressed GFP-LC3 in MCF-7 cells and then incubated them with partially purified extracts from our natural product collection derived from traditional Chinese medicinal herbs. We also incubated the cells with DMSO alone and with tamoxifen as negative and positive controls, respectively. We analyzed the images in individual wells captured by fluorescent microscopy and quantified the levels of autophagy. We found that a partially purified fraction from the rhizome of *Alisma orientale* consistently upregulated the percentage of cells exhibiting GFP-LC3 puncta (Supplementary Fig. S1). The fraction was subjected to further bioactivity-guided purification using repeated flash column chromatography on silica gel and normal and reverse-phase preparative high performance liquid chromatography. Finally, the compounds in the purified active fraction were deduced by comparing their ^{1}H and ^{13}C nuclear magnetic resonance spectroscopic data with those of known *Alisma* components (22, 23) and were identified to be alisol A 23-acetate and alisol A 24-acetate (Fig. 1A), compounds that are known to interconvert rapidly (24). Cytotoxicity was also observed by these compounds upon incubation with the cells.

Alisol B Induces Autophagy and Cell Death toward Cancer Cell Lines

To confirm the observed activity for inducing autophagy and cell death, four structurally related alisol derivatives, including alisol A 24-acetate, alisol B 23-acetate, alisol A, and alisol B (Fig. 1A), were obtained commercially and their cytotoxicities toward a panel of cancer cell lines were evaluated, respectively. Among these, alisol B 23-acetate and alisol B displayed similar cytotoxicities against tumor cells of different origins (Table 1). Alisol A 24-acetate exhibited a lower cytotoxicity, whereas alisol A is comparatively inactive. To evaluate the potency of these compounds for the induction of autophagy, MCF-7 cells were treated with each of the four compounds at their respective IC_{50} and the formation of GFP-LC3 puncta were evaluated. GFP-LC3 puncta were significantly increased in the presence of all of the compounds except alisol A (Fig. 1B).

Among the three active compounds, alisol B was the most active while having the simplest pharmacophore required for the observed biological activities. Moreover, alisol B is relatively stable and is the most abundant alisol derivative in the alcohol extract of *Alisma orientale* (25). Therefore, it was selected as a model to characterize the molecular mechanism of action for this class of compounds.

Besides MCF-7 cells, alisol B also induced the formation of GFP-LC3 puncta in a variety of cell lines examined

(Supplementary Fig. S2), demonstrating that this compound was able to induce autophagy in a broad spectrum of cell types. The ultrastructures of alisol B–treated MCF-7 cells were analyzed by transmission electron microscopy. Numerous autophagosomes characterized by double membrane structures were detected in cells treated with alisol B (30 μmol/L) and autophagic vacuoles containing degraded organelles were also identified (Fig. 2A). We then measured LC3-II formation in the presence of lysosomal protease inhibitors (26). Whereas alisol B or lysosomal protease inhibitors alone increased the level of LC3-II as expected, alisol B significantly increased the rate of LC3-II formation in the presence of the inhibitors, compared with the use of protease inhibitors alone (Fig. 2B), suggesting that alisol B induces autophagic activity as a result of enhanced autophagosome formation.

Next, the effect of alisol B on cell cycle progression was investigated. Alisol B induced a time-dependent accumulation of cells in the G_1 phase, with a concomitant reduction in the S and G_2-M phases, respectively (Table 2). Alisol B also leads to a gradual accumulation of p27 in several cell lines (Fig. 2C). Taken together, these data suggested that alisol B induces cell cycle arrest at the G_1 phase before inducing cell death.

Alisol B Induces Autophagy through the Activation of CaMKK-AMPK-mTOR Kinase Signaling Cascade

Nutrient deprivation activates autophagy through an mTOR-dependent pathway, in which the 5′-AMP–activated protein kinase (AMPK) phosphorylates and activates TSC2, leading to the inactivation of mTOR (27). HeLa (data not shown) and MCF-7 cells treated with alisol B showed a time-dependent increase in AMPK phosphorylation at Thr172 (Fig. 3A), accompanied by a concomitant reduction in phosphorylated p70S6K, a downstream target of mTOR. On the other hand, a significant reduction in alisol B–induced GFP-LC3 puncta formation (Fig. 3B) was observed in cells pretreated with compound C, an AMPK inhibitor. Collectively, these data suggested that alisol B induces autophagy through the mTOR pathway in an AMPK-dependent manner.

Autophagy can be induced by Ca^{2+} mobilizing agents through the CaMKKβ-AMPK-mTOR signaling cascade (28). To elucidate the involvement of CaMKK in alisol B–induced autophagy, cells were treated with alisol B in the presence of STO-609, a CaMKK inhibitor (29). STO-609 inhibited the alisol B–induced phosphorylation of AMPK (Fig. 3C) and significantly reduced the percentage of cells exhibiting GFP-LC3 puncta (Supplementary Fig. S3A; Fig. 3D). Consistently, the addition of intracellular Ca^{2+} chelator (BAPTA/AM) to cells abolished the formation of GFP-LC3 puncta (Supplementary Fig. S3B; Fig. 3E). Importantly, BAPTA/AM also significantly inhibited alisol B–induced cell death (Fig. 3F). Taken together, these data suggested that alisol B induces autophagy by increasing the release of free cytosolic calcium ($[Ca^{2+}]c$) from intracellular stores, and implicates the role of $[Ca^{2+}]c$ in alisol B–induced cell death.

Alisol B Induced UPR and Apoptotic Cell Death

Several anticancer therapeutics can induce autophagy in cancer cells (9), but it remains controversial as to whether autophagy is the driver of cell death or a prosurvival process in response to drug treatment. To determine the role of autophagy in alisol B–induced cell death, cells were either treated with 3-MA, a known class III phosphatidylinositol-3′-kinase inhibitor, or with RNAi against beclin1 to block autophagy before alisol B treatment. Although 3-MA significantly reduced cell death induced by alisol B (Fig. 4A), the gene knockdown of beclin1 failed to rescue cells from alisol B–induced cell death (Fig. 4B). These apparently contradictory findings prompted us to further investigate the role of autophagy in alisol B–induced cell death using ATG7-deficient mouse embryonic fibroblasts, which is resistant to autophagic induction (30). As shown in Fig. 4C, $ATG7^{-/-}$ cells were more sensitive to alisol B–induced cell death compared with the wild-type cells, implicating that cells activate autophagy in response to alisol B as an adaptive mechanism for cell survival.

The apparent contradictory results obtained by pharmacologic inhibition and gene silencing/knockout of autophagic pathway could be explained by a recent report that showed that UPR can be blocked by 3-MA (30). Because our data showed that alisol B induces calcium mobilization, which is known to cause ER stress, UPR activation (31), and apoptosis (32), 3-MA might therefore promote cell survival through suppressing alisol B–induced UPR activation. To explore this possibility, the effect of alisol B on known components of the UPR process including the activation of PERK, IRE1, and the activation of transcription factor-6 (ATF6) signaling pathways was determined. Similar to the action of thapsigargin, a known autophagy inducer, ER stress inducer, and Ca^{2+} mobilizer, alisol B induced PERK and eIF2α phosphorylation in cells. This was accompanied by an induction of ATF4, ER molecular chaperone BiP/GRP78, and CHOP expression (Fig. 5A), suggesting that the PERK signaling pathway was activated by alisol B treatment. On the other hand, thapsigargin, but not alisol B, induced the splicing of Xbp-1 mRNA, suggesting that alisol B did not activate the IRE1 pathway (Fig. 5B). Finally, alisol B induced the activity of the ATF6 reporter gene similar to that of thapsigargin, suggesting that the ATF6 pathway was also activated (Fig. 5C). Together, these data suggested that alisol B activates UPR through the PERK and ATF6 signaling pathways. In addition, we confirmed that alisol B–induced cell death is mediated by apoptosis as measured by binding to Annexin V and 7-ADD (Table 3) and the cleavage of poly ADP ribose polymerase (Fig. 5D), respectively.

SERCA Pump Is a Potential Molecular Target for Alisol B

Because the biological action of alisol B resembled thapsigargin, a potent inhibitor of the SERCA pump, which induces autophagy and UPR through perturbing calcium

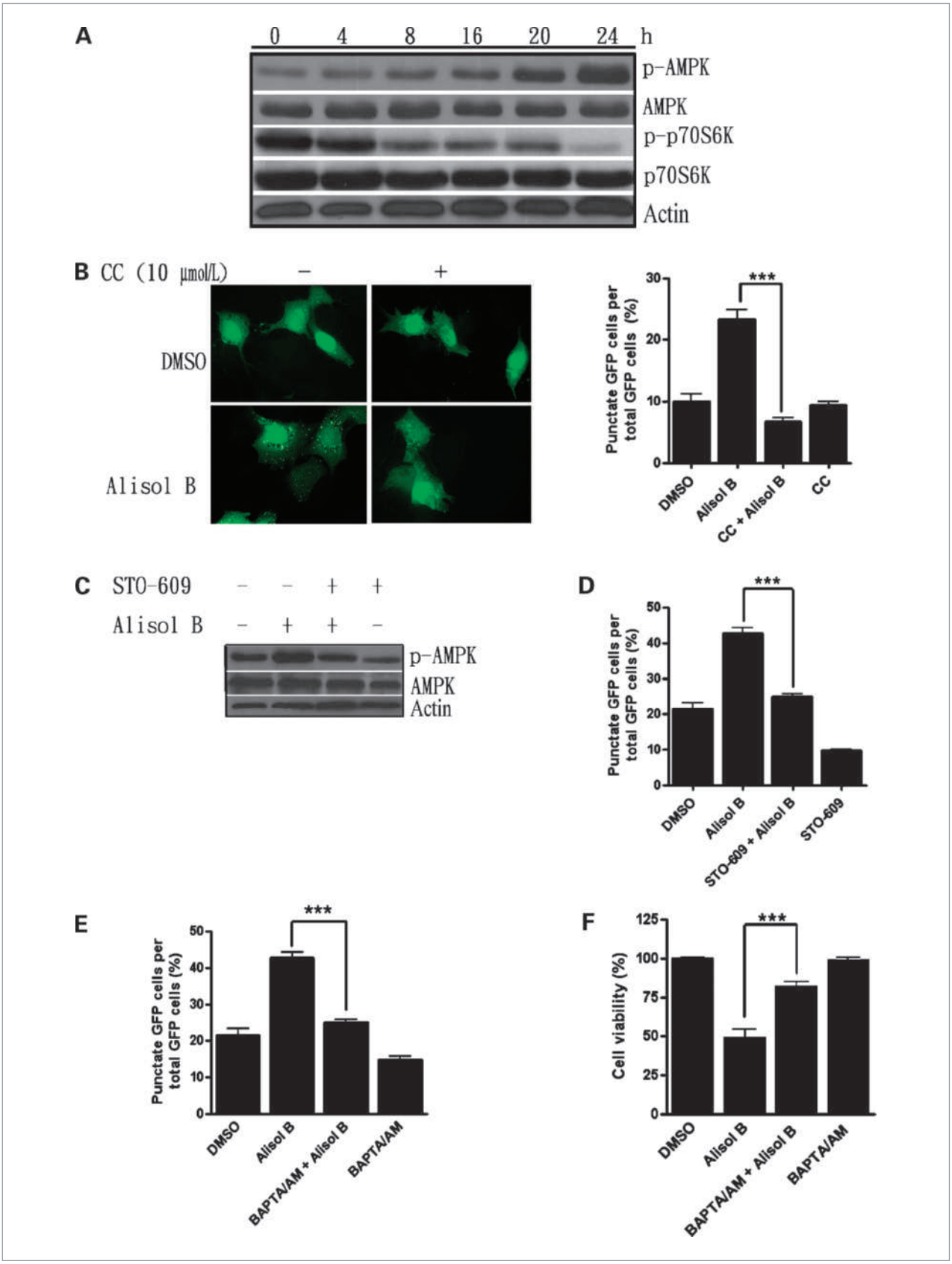

homeostasis (28), we postulated that alisol B might also function as a SERCA pump inhibitor. We therefore carried out computational virtual ligand docking studies to evaluate the molecular interactions between alisol B and SERCA1A. Comparative analysis of the low-energy ligand conformations found the preferred site for alisol B to be within the transmembrane domain (Fig. 6A), similar to that found for thapsigargin (31), with a strong binding interaction as reflected by the score of −30.7. As a reference, molecular docking of the known SERCA pump inhibitor thapsigargin showed a score of −32. The top-scoring binding pose of alisol B is characterized by the protostane tetracycle residing in a hydrophobic pocket, being in close contact with amino acid residues Phe256, Val263, Ile765, Val769, whereas the OH group of alisol B is pointing toward Lys252 and Glu255 and having a direct hydrogen bond with the carboxylate of Glu255. An overlay of the low-energy pose of alisol B and thapsigarin with the SERCA pump is also shown (Fig. 6B). On the other hand, consistent with the biological activity, alisol A showed unfavorable interactions with the active site (binding score = −16.68; Supplementary Fig. S4).

To ascertain whether the SERCA pump was inhibited by alisol B, we measured its effect using both purified rabbit skeletal muscle sarcoplasmic reticulum (SR) membranes, which express the SERCA1A isoforms and porcine brain microsomes, which express mainly SERCA2B (33). SERCA2B is the most abundantly found SERCA isoforms in nonmuscle cells and therefore is likely to be a major isoform in the cells lines used. It should also be noted that SERCA1A and SERCA2B are highly conserved between mammalian species (i.e., SERCA1A has a 97% sequence identity between human and rabbit, whereas SERCA2B has a 99% sequence identity between human and pig). As shown in Fig. 6C, the SERCA1A pump (from rabbit skeletal muscle SR) was inhibited by alisol B in a dose-dependent manner, which was fitted to an allosteric dose versus effect equation (see Supplementary Table S1 for details; IC_{50}, 27 ± 5 μmol/L), whereas alisol A exhibited a much lower inhibitory effect (IC_{50}, 100 ± 30 μmol/L; full details of the curve fitting parameters are given in Supplementary Table S1). Figure 6D shows the effects of thapsigargin on Ca^{2+} ATPase activity when measured in rabbit skeletal muscle SR membranes and pig brain microsomes. Thapsigargin is an extremely potent SERCA inhibitor, exhibiting IC_{50} values of 40 ± 7 nmol/L for SR membranes and 11 ± 1 nmol/L for brain microsomes, respectively. Consistent with our previous findings, the inhibition of activity approaches completion in SR membranes but plateaus in brain microsomes such that ~30% of the measured Ca^{2+} ATPase activity remains unaffected (Supplementary Table S1; refs. 34, 35). We have since shown that this residual activity in brain microsomes is due to the presence of another Ca^{2+} ATPase known as SPCA, which is insensitive to thapsigargin as well as some other SERCA inhibitors (35, 36). Figure 6E shows the Ca^{2+} ATPase inhibition curves for alisol A and B when measured in brain microsomes. Again, both sets of data fitted to the allosteric equation, again showing that in these membranes, ~30% of the activity was insensitive to the alisols as observed for thapsigargin (Supplementary Table S1). The results showed that alisol B was again a more potent SERCA2B inhibitor compared with alisol A (IC_{50}, 53 ± 6 μmol/L and 140 ± 25 μmol/L, respectively). The fact that alisol B is slightly more potent for SERCA1A compared with SERCA2B is consistent with the findings for thapsigargin, which is also more potent for SERCA1A than SERCA2B (37). The IC_{50} values of alisol A and B toward both isoforms of the SERCA pump were concordant with the IC_{50} values for their respective cytotoxicities and calculated binding scores. Collectively, our data strongly suggested that alisol B is a novel SERCA pump inhibitor.

Discussion

Using an image-based screen, alisol A 23-acetate was purified and identified to be a modest inducer of autophagy and cell death. The alisols are triterpene compounds that belong to the protostane family and are known bioactive components of the rhizomes of *Alisma orientale* (38). Despite alisol derivatives having been reported to possess a range of biological activities, including the inhibition of nitric oxide synthesis (39), the inhibition of HBV replication (40), the induction of cell death in tumor cells (23, 41), and the reversal of multidrug resistance (42), the underlying mechanisms and the molecular targets of these compounds have remained elusive.

Here, using alisol B as a model drug for this family of compounds, we showed that it induces calcium mobilization from internal stores, leading to the activation of autophagy through the CaMKK-AMPK-mTOR pathway. We further showed that the disturbance of calcium

Figure 3. Alisol B activates the CaMKKβ-AMPK-TOR signaling pathway. A, MCF-7 cells were treated with alisol B (30 μmol/L) and analyzed using the indicated antibodies. B, MCF-7 cells expressing GFP-LC3 were treated with alisol B (30 μmol/L) or DMSO in the presence or absence of compound C (CC, 10 μmol/L) for 16 h. Left, representative pictures with punctate GFP-LC3 fluorescence. Right, bar chart showing the percentage of GFP-positive cells with GFP-LC3 puncta under these treatments. C, MCF-7 cells were treated with alisol B in the presence or absence of STO-609 (25 μmol/L) for 16 h. Cell lysates were analyzed for p-AMPK, AMPK, and β-actin, respectively. D, MCF-7 cells expressing GFP-LC3 were treated with DMSO or alisol B in the presence or absence of STO-609. Bar chart showing the percentage of GFP-positive cells with GFP-LC3 puncta under these treatments. E, MCF-7 cells expressing GFP-LC3 were treated with DMSO or alisol B in the presence or absence of BAPTA/AM (25 μmol/L). Bar chart showing the percentage of GFP-positive cells with GFP-LC3 puncta under these treatments. F, cell viability of MCF-7 cells treated with alisol B (30 μmol/L) in the presence or absence of 25 μmol/L BAPTA/AM. Cell viability was measured by MTT assay. Columns, means of three independent experiments; bars, SEM. ***, $P < 0.001$.

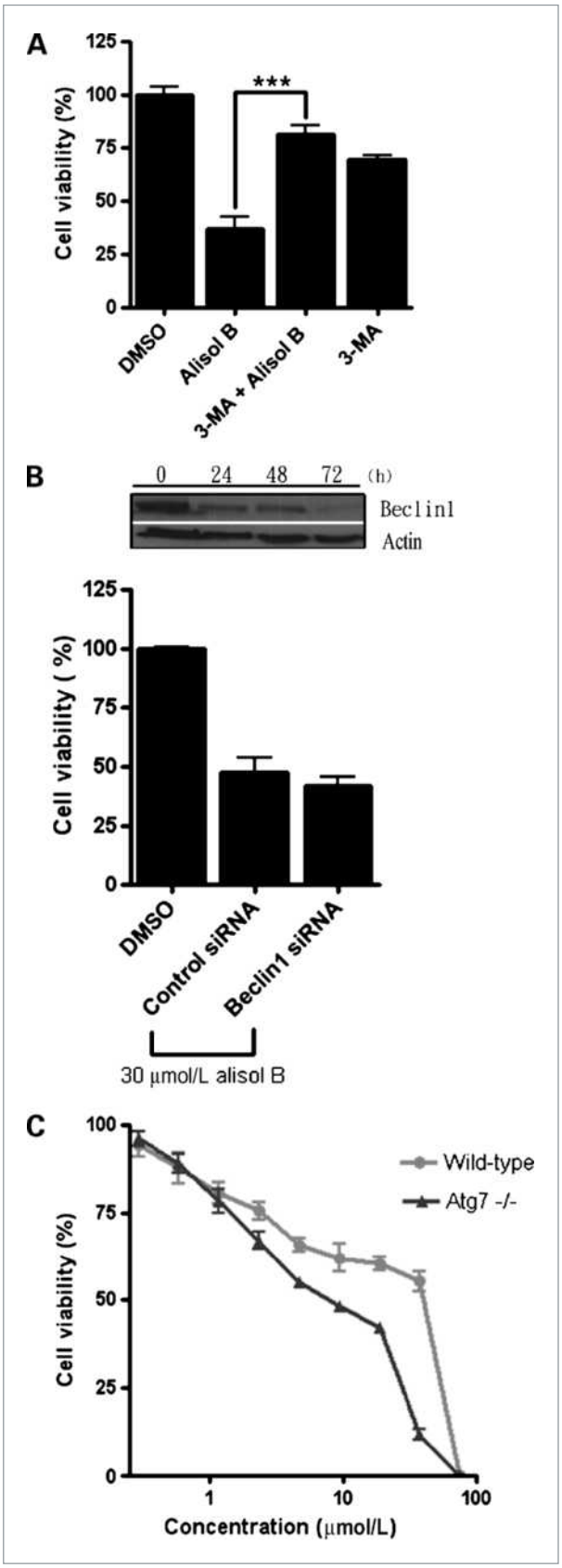

homeostasis by alisol B activates UPR and apoptotic cell death. In contrast to some compounds that induce autophagic cell death (11), our findings suggested that autophagic induction in alisol B–treated cells is a pro-survival mechanism. Our conclusion is supported by the observations that genetic ablation of genes beclin1 and ATG7 in the autophagic pathway rendered cells more susceptible to the cytotoxicity of alisol B. Finally, we provided evidence that alisol B inhibited the activity of the SERCA pump, whereas alisol A is far less active.

Although alisol B 23 acetate has been found to be as effective as alisol B in the induction of autophagy and cell death, it is possible that in the cell-based assays, cell esterases catalyzed the hydrolysis of alisol B 23 acetate to generate alisol B; thus, alisol B is the actual active compound in both sets of experiments. This is corroborated by the docking studies that identified the OH group in alisol B acting as a hydrogen bond donor as one of the interactions within the binding site, which is not possible when the OH group is acetylated as in the alisol B 23 acetate. On the other hand, the higher activity of alisol B over alisol A could only be attributed to the presence of the epoxide in alisol B instead of a vicinal diol in alisol A. The epoxide functional group in alisol B contributes to the overall bioactivity by inducing a different orientation and conformation of the side chain, particularly at C23-C24-C25, and renders the terminus of alisol B more compact to fit into the binding site compared with alisol A. Although the reactivity of the epoxide allows the possibility of nucleophiles to attack and result in covalent bonding with SERCA, the examination of the pocket showed it to be a relatively hydrophobic region and did not reveal any obvious nucleophiles. Whether the binding of alisol B with SERCA is indeed irreversible could be determined experimentally by additional competition experiments in the future.

The SERCA pump has been explored as a potential target in cancer. Inhibition of SERCA triggers cell death in several cancer cells (43, 44). Thapsigargin is the most selective and potent inhibitor of the SERCA pump. It is a sesquiterpene lactone natural product extracted from the umbelliferous plant *Thapsia garganica*, which inhibits all the SERCA isoenzymes at subnanomolar potencies. Thapsigargin blocks the uptake of calcium into the sarcoplasmic and endoplasmic reticula, leading to calcium depletion in these stores and increase in cytosolic calcium.

Figure 4. A, cell viability of MCF-7 cells treated with alisol B (30 μmol/L) in the presence or absence of 3-MA (10 mmol/L) for 48 h. B, top, MCF-7 cells were transfected with small interfering RNAs (siRNA) against beclin1 for the indicated times. Cell lysates were analyzed by Western blot for the expression of beclin1 using antibodies. Bottom, cell viability of MCF-7 cells transfected with beclin1 or nontargeting (control) small interfering RNAs for 24 h before the addition of alisol B for an additional 48 h. Cell viability was measured by MTT assay. C, cytotoxicity of alisol B on wild-type and ATG7$^{-/-}$ mouse embryonic fibroblasts as measured by the MTT assay. Points, mean of three independent experiments; bars, SEM.

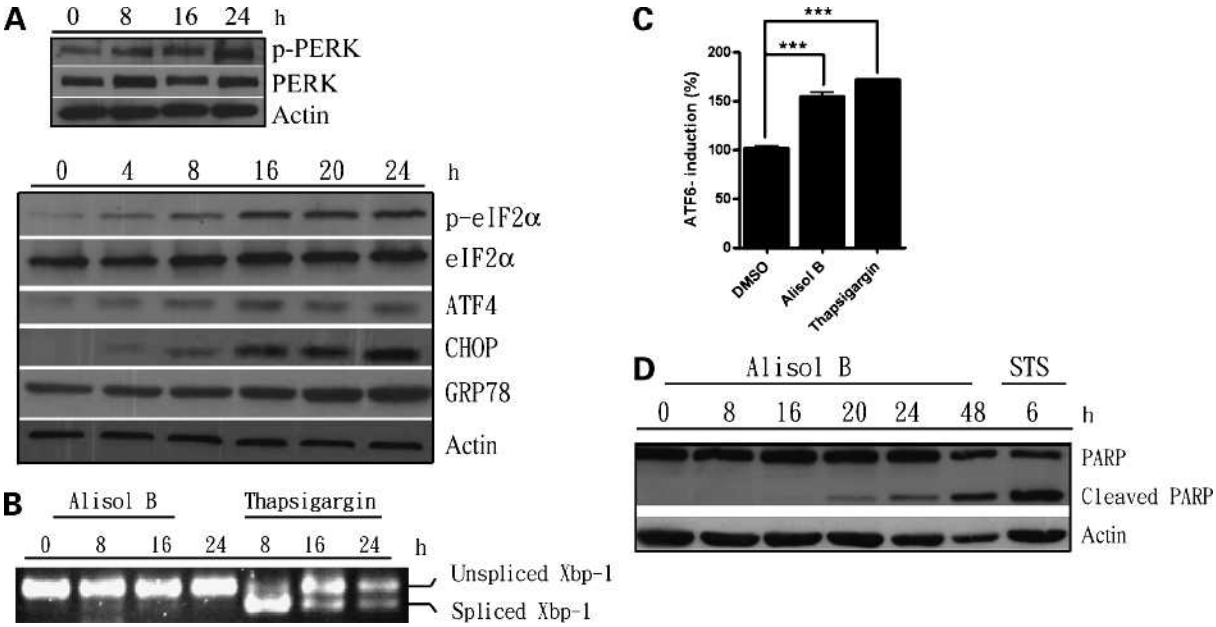

Figure 5. Alisol B induces UPR and apoptotic cell death. A, MCF-7 cells were treated with alisol B (30 μmol/L) for the indicated times. Cell lysates were analyzed for p-PERK, PERK, p-eIF2α, eIF2α, ATF4, CHOP, GRP78, and β-actin, respectively. B, MCF-7 cells were treated with alisol B (30 μmol/L) or thapsigargin (1 μmol/L) for the indicated time. Reverse transcription-PCR was carried out to analyze Xbp-1 mRNA splicing. C, MCF-7 cells were transfected with pATF6-Luc and pCMV-*Renilla* luciferase reporter constructs, and treated with DMSO, alisol B, or thapsigargin for 24 h, respectively. Firefly and *Renilla* luciferase activities were measured. Normalized luciferase activity was shown relative to DMSO treatment. D, MCF-7 cells were treated with alisol B (30 μmol/L) for the indicated times and analyzed by poly ADP ribose polymerase (PARP) and β-actin antibodies. Staurosporine (STS, 1 μmol/L) was used as positive control. Columns, means of three independent experiments; bars, SEM.

It is believed that the perturbation of calcium homeostasis by thapsigargin disrupts protein folding and activates all three arms of UPR, respectively (45, 46). Furthermore, thapsigargin-mediated increase in intracellular calcium also plays an important role in the activation of autophagy (28) and calpain-mediated apoptosis (43). Although thapsigargin is toxic toward both normal and tumor cells, it is particularly effective in targeting tumor cells with low proliferative indices such as prostate cancer. Accordingly, a thapsigargin analogue that is only activated by the prostate-specific antigen has shown efficacy in experimental prostate cancer models with no discernable toxicity (47).

Several compounds, including the cyclooxygenase-2 inhibitor celecoxib (48) and curcumin (36), are also known to possess antitumor activity as least partially ascribed to their inhibitory activity toward SERCA. Being a SERCA inhibitor, alisol B elicited a range of cellular responses resembling, but not identical, to that of thapsigargin. Our findings therefore suggest that alisol B can be further exploited as a cancer therapeutic by a prodrug strategy similar to that of thapsigargin. Although alisol B induced a disturbance of calcium homeostasis, autophagy, and ER stress, it activated only the PERK and ATF6 arms of the UPR pathway, while sparing the IRE1 pathway. It has been shown that although the PERK, ATF6, and IRE1

Table 3. MCF-7 cells treated with alisol B for the indicated times were subjected to Annexin V and 7-ADD assay using flow cytometry

Time (h)	Viable Annexin V-7AAD-	Early apoptosis Annexin V+ 7AAD-	Late apoptosis Annexin V+ 7AAD+	Necrosis Annexin V- 7AAD+
0	90.6 ± 1.4	2.5 ± 0.5	6.3 ± 1.3	0.6 ± 0.2
24	86.7 ± 1.9	2.0 ± 0.4	8.5 ± 1.9	2.7 ± 0.7
48	54.0 ± 1.3	3.8 ± 0.2	36.9 ± 1.3	5.3 ± 1.2

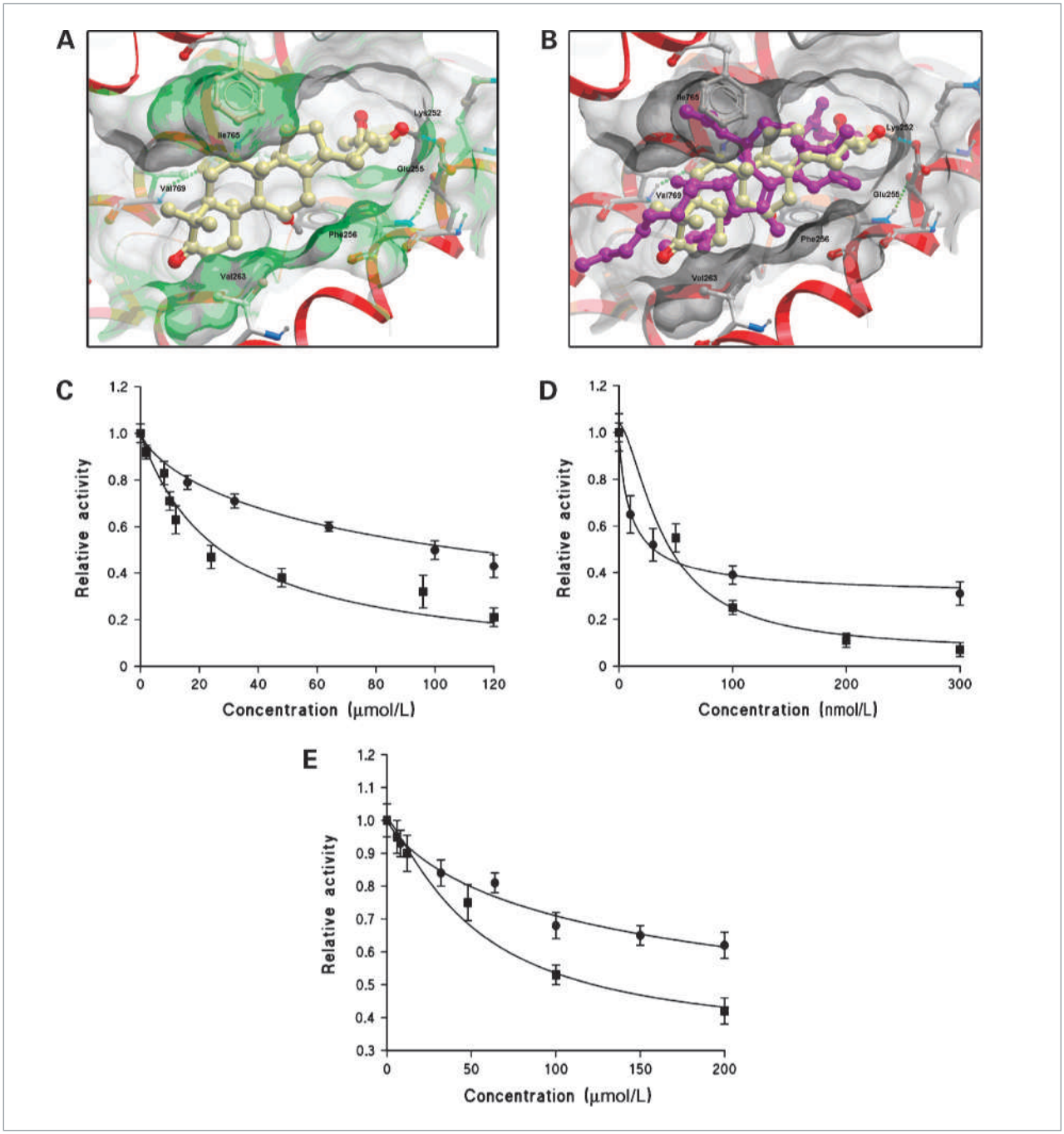

Figure 6. A, minimized energy pose of alisol B in SERCA1A pump. Stick model, alisol B; yellow, carbon; red, oxygen. B, overlay of low-energy pose of alisol B (yellow, carbon; gray, hydrogen; red, oxygen; blue, nitrogen) and thapsigargin (purple) with the SERCA pump (depicted in ribbon form and colored red). C to E, inhibition of SERCA isoforms by alisols. C, the inhibition of Ca^{2+} ATPase activity in skeletal muscle SR by alisol A (●) and alisol B (■). Experiments were measured at 25°C (pH 7.2) using the coupled enzyme assay as described in ref. 21. D, the thapsigargin inhibition of Ca^{2+} ATPase activity using membranes derived from skeletal muscle SR (■) and brain microsomes (●). E, the effects of alisol A (●) and alisol B (■) on the Ca^{2+} ATPase activity measured in brain microsomes as described in ref. 21. Points, mean of 3 to 5 replicates; bars, SEM. The curves are the best fits to the experimental data using the noncompetitive equation (goodness-of-fit to all the inhibition data (χ^2) was >0.97).

signaling pathways are activated by UPR, persistent activation of the PERK signaling pathway, coupled with the rapid attenuation of IRE1 and ATF6 activities, are required for the execution of apoptosis (49), whereas extended activation of IRE1 signaling promotes cell survival instead (50). Therefore, the unique pharmacologic property of alisol B may confer an advantage with regard to the induction of apoptotic cell death. Although the

mechanistic basis behind this observation remains elusive, it is possible that alisol B may also be an inhibitor of the IRE1 signaling cascade. To our knowledge, alisol B is the only SERCA inhibitor known to selectively promote UPR induction. Although a relatively high dosage is required for alisol B to exert its effect, this could probably be improved by modification of the parental compound by rational drug design in the future. Accordingly, we have developed a novel purification procedure for the large-scale extraction of alisol B from *Alismatis orientale* recently.[7] This would allow an ample supply of the compound for future *in vivo* animal testing and synthesis of structural analogues for structure-activity relationship analysis.

[7] Chiu and Ko, unpublished data.

Disclosure of Potential Conflicts of Interest

No potential conflicts of interest were disclosed.

Acknowledgments

We thank Janet Tam for the help in transmission electron microscopy, and Lai-To Leung, Alan Y. L. Chan, John C. K. Chu, and Mina M. T. Ip for help in the extraction and purification of the TCM herbal components.

Grant Support

University Grants Committee of the Hong Kong Special Administrative Region Areas of Excellence Scheme grant AoE/P-10/01 and University of Hong Kong Generic Drugs Research Program.

The costs of publication of this article were defrayed in part by the payment of page charges. This article must therefore be hereby marked *advertisement* in accordance with 18 U.S.C. Section 1734 solely to indicate this fact.

Received 07/30/2009; revised 01/14/2010; accepted 01/14/2010; published OnlineFirst 03/02/2010.

References

1. Levine B, Klionsky DJ. Development by self-digestion: molecular mechanisms and biological functions of autophagy. Dev Cell 2004;6:463–77.
2. Mizushima N. Autophagy: process and function. Genes Dev 2007;21:2861–73.
3. Mathew R, Kongara S, Beaudoin B, et al. Autophagy suppresses tumor progression by limiting chromosomal instability. Genes Dev 2007;21:1367–81.
4. Liang XH, Jackson S, Seaman M, et al. Induction of autophagy and inhibition of tumorigenesis by beclin 1. Nature 1999;402:672–6.
5. Melendez A, Talloczy Z, Seaman M, Eskelinen EL, Hall DH, Levine B. Autophagy genes are essential for dauer development and life-span extension in C. elegans. Science 2003;301:1387–91.
6. Tsujimoto Y, Shimizu S. Another way to die: autophagic programmed cell death. Cell Death Differ 2005;12 Suppl 2:1528–34.
7. Ravikumar B, Vacher C, Berger Z, et al. Inhibition of mTOR induces autophagy and reduces toxicity of polyglutamine expansions in fly and mouse models of Huntington disease. Nat Genet 2004;36:585–95.
8. Sarkar S, Perlstein EO, Imarisio S, et al. Small molecules enhance autophagy and reduce toxicity in Huntington's disease models. Nat Chem Biol 2007;3:331–8.
9. Kondo Y, Kanzawa T, Sawaya R, Kondo S. The role of autophagy in cancer development and response to therapy. Nat Rev Cancer 2005;5:726–34.
10. Hoyer-Hansen M, Bastholm L, Mathiasen IS, Elling F, Jaattela M. Vitamin D analog EB1089 triggers dramatic lysosomal changes and Beclin 1-mediated autophagic cell death. Cell Death Differ 2005;12:1297–309.
11. Chang CP, Yang MC, Liu HS, Lin YS, Lei HY. Concanavalin A induces autophagy in hepatoma cells and has a therapeutic effect in a murine *in situ* hepatoma model. Hepatology 2007;45:286–96.
12. Opipari AW, Jr., Tan L, Boitano AE, Sorenson DR, Aurora A, Liu JR. Resveratrol-induced autophagocytosis in ovarian cancer cells. Cancer Res 2004;64:696–703.
13. Chin KT, Zhou HJ, Wong CM, et al. The liver-enriched transcription factor CREB-H is a growth suppressor protein underexpressed in hepatocellular carcinoma. Nucleic Acids Res 2005;33:1859–73.
14. Wong VK, Chiu P, Chung SS, et al. Pseudolaric acid B, a novel microtubule-destabilizing agent that circumvents multidrug resistance phenotype and exhibits antitumor activity *in vivo*. Clin Cancer Res 2005;11:6002–11.
15. Shang J, Lehrman MA. Discordance of UPR signaling by ATF6 and Ire1p-XBP1 with levels of target transcripts. Biochem Biophys Res Commun 2004;317:390–6.
16. Totrov M, Abagyan R. Flexible protein-ligand docking by global energy optimization in internal coordinates. Proteins 1997;Suppl 1:215–20.
17. Schapira M, Totrov M, Abagyan R. Prediction of the binding energy for small molecules, peptides and proteins. J Mol Recognit 1999;12:177–90.
18. Michelangeli F, Munkonge FM. Methods of reconstitution of the purified sarcoplasmic reticulum (Ca(2+)-Mg2+)-ATPase using bile salt detergents to form membranes of defined lipid to protein ratios or sealed vesicles. Anal Biochem 1991;194:231–6.
19. Michelangeli F, Colyer J, East JM, Lee AG. Effect of pH on the activity of the Ca2+ + Mg2(+)-activated ATPase of sarcoplasmic reticulum. Biochem J 1990;267:423–9.
20. Mezna M, Michelangeli F. The effects of inositol 1,4,5-trisphosphate (InsP3) analogues on the transient kinetics of Ca2+ release from cerebellar microsomes. InsP3 analogues act as partial agonists. J Biol Chem 1996;271:31818–23.
21. Longland CL, Mezna M, Langel U, et al. Biochemical mechanisms of calcium mobilisation induced by mastoparan and chimeric hormone-mastoparan constructs. Cell Calcium 1998;24:27–34.
22. Nakajima Y, Satoh Y, Katsumata M, Tsujiyama K, Ida Y, Shoji J. Terpenoids of Alisma orientale rhizome and the crude Drug Alismatis rhizoma. Phytochemistry 1994;36:119–27.
23. Lee S, Min B, Bae K. Chemical modification of alisol B 23-acetate and their cytotoxic activity. Arch Pharm Res 2002;25:608–12.
24. Makabel B, Zhao Y, Wang B, et al. Stability and structure studies on alisol a 24-acetate. Chem Pharm Bull (Tokyo) 2008;56:41–5.
25. Kubo M, Matsuda H, Tomohiro N, Yoshikawa M. Studies on Alismatis rhizoma. I. Anti-allergic effects of methanol extract and six terpene components from Alismatis rhizoma (dried rhizome of Alisma orientale). Biol Pharm Bull 1997;20:511–6.
26. Mizushima N, Yoshimori T. How to interpret LC3 immunoblotting. Autophagy 2007;3:542–5.
27. Mizushima N, Klionsky DJ. Protein turnover via autophagy: implications for metabolism. Annu Rev Nutr 2007;27:19–40.
28. Hoyer-Hansen M, Bastholm L, Szyniarowski P, et al. Control of macroautophagy by calcium, calmodulin-dependent kinase kinase-β, and Bcl-2. Mol Cell 2007;25:193–205.
29. Tokumitsu H, Inuzuka H, Ishikawa Y, Ikeda M, Saji I, Kobayashi R. STO-609, a specific inhibitor of the Ca(2+)/calmodulin-dependent protein kinase kinase. J Biol Chem 2002;277:15813–8.

30. Li J, Ni M, Lee B, Barron E, Hinton DR, Lee AS. The unfolded protein response regulator GRP78//BiP is required for endoplasmic reticulum integrity and stress-induced autophagy in mammalian cells. Cell Death Differ 2008;15:1460–71.
31. Hoyer-Hansen M, Jaattela M. Connecting endoplasmic reticulum stress to autophagy by unfolded protein response and calcium. Cell Death Differ 2007;14:1576–82.
32. Schroder M. Endoplasmic reticulum stress responses. Cell Mol Life Sci 2008;65:862–94.
33. Wu KD, Lee WS, Wey J, Bungard D, Lytton J. Localization and quantification of endoplasmic reticulum Ca(2+)-ATPase isoform transcripts. Am J Physiol 1995;269:C775–84.
34. Brown GR, Benyon SL, Kirk CJ, et al. Characterisation of a novel Ca2+ pump inhibitor (bis-phenol) and its effects on intracellular Ca2+ mobilization. Biochim Biophys Acta 1994;1195:252–8.
35. Wootton LL, Argent CC, Wheatley M, Michelangeli F. The expression, activity and localisation of the secretory pathway Ca2+-ATPase (SPCA1) in different mammalian tissues. Biochim Biophys Acta 2004;1664:189–97.
36. Bilmen JG, Khan SZ, Javed MH, Michelangeli F. Inhibition of the SERCA Ca2+ pumps by curcumin. Curcumin putatively stabilizes the interaction between the nucleotide-binding and phosphorylation domains in the absence of ATP. Eur J Biochem 2001;268: 6318–27.
37. Wootton LL, Michelangeli F. The effects of the phenylalanine 256 to valine mutation on the sensitivity of sarcoplasmic/endoplasmic reticulum Ca2+ ATPase (SERCA) Ca2+ pump isoforms 1, 2, and 3 to thapsigargin and other inhibitors. J Biol Chem 2006;281:6970–6.
38. Murata T, Imai Y, Hirata T, Miyamoto M. Biological-active trieterpenes of Alismatis rhizoma. I. Isolation of the alisols. Chem Pharm Bull (Tokyo) 1970;18:1347–53.
39. Kim NY, Kang TH, Pae HO, et al. *In vitro* inducible nitric oxide synthesis inhibitors from Alismatis Rhizoma. Biol Pharm Bull 1999; 22:1147–9.
40. Zhang Q, Jiang ZY, Luo J, et al. Anti-HBV agents. Part 2: Synthesis and *in vitro* anti-hepatitis B virus activities of alisol A derivatives. Bioorg Med Chem Lett 2009;19:2148–53.
41. Huang YT, Huang DM, Chueh SC, Teng CM, Guh JH. Alisol B acetate, a triterpene from Alismatis rhizoma, induces Bax nuclear translocation and apoptosis in human hormone-resistant prostate cancer PC-3 cells. Cancer Lett 2006;231:270–8.
42. Wang C, Zhang J-X, Shen X-L, Wan C-K, Tse AK-W, Fong W-F. Reversal of P-glycoprotein-mediated multidrug resistance by Alisol B 23-acetate. Biochem Pharmacol 2004;68:843–55.
43. Furuya Y, Lundmo P, Short AD, Gill DL, Isaacs JT. The role of calcium, pH, and cell proliferation in the programmed (apoptotic) death of androgen-independent prostatic cancer cells induced by thapsigargin. Cancer Res 1994;54:6167–75.
44. He Q, Lee DI, Rong R, et al. Endoplasmic reticulum calcium pool depletion-induced apoptosis is coupled with activation of the death receptor 5 pathway. Oncogene 2002;21:2623–33.
45. Haze K, Yoshida H, Yanagi H, Yura T, Mori K. Mammalian transcription factor ATF6 is synthesized as a transmembrane protein and activated by proteolysis in response to endoplasmic reticulum stress. Mol Biol Cell 1999;10:3787–99.
46. Urano F, Wang X, Bertolotti A, et al. Coupling of stress in the ER to activation of JNK protein kinases by transmembrane protein kinase IRE1. Science 2000;287:664–6.
47. Denmeade SR, Jakobsen CM, Janssen S, et al. Prostate-specific antigen-activated thapsigargin prodrug as targeted therapy for prostate cancer. J Natl Cancer Inst 2003;95:990–1000.
48. Johnson AJ, Hsu AL, Lin HP, Song X, Chen CS. The cyclooxygenase-2 inhibitor celecoxib perturbs intracellular calcium by inhibiting endoplasmic reticulum Ca2+-ATPases: a plausible link with its anti-tumour effect and cardiovascular risks. Biochem J 2002;366: 831–7.
49. Lin JH, Li H, Yasumura D, et al. IRE1 signaling affects cell fate during the unfolded protein response. Science 2007;318:944–9.
50. Lin JH, Li H, Zhang Y, Ron D, Walter P. Divergent effects of PERK and IRE1 signaling on cell viability. PLoS ONE 2009;4:e4170.